Dronning Maud Land (Antarctica) and Reconstruction of Its Glacial History with Cosmogenic Radionuclides

Waseem Ahmad Baba, Pankaj Kumar, Jitendra Kumar Pattanaik, and Neloy Khare

Abstract This chapter deliberates Dronning Maud Land's glacial history (DML) based on available dates obtained using cosmogenic radionuclides. As Dronning Maud Land is a part of the East Antarctica Ice Sheet (EAIS), background information about EAIS and its glacial history is also discussed based on the researchers' various evidence. A comprehensive outline of DML, the basics of cosmogenic radionuclide and its application and major glacial events from DML are presented in this chapter. Further, meltwater's pulse due to deglaciation of EAIS and evidence related to the marine isotope stages were discussed to understand the impact of deglaciation on the global ocean. A very few direct dates were available from Dronning Maud Land to establish the detailed glacial chronology, or some of the results are contradicting. This region shows sparse or no evidence of ice thickening during the last glacial maximum (LGM). Field observations and ice core models show that the ice sheet's interior parts, the ice dome, were possibly 100 m lower during LGM than the present. The results obtained by the various researchers shows that around 600 m high ice sheet existed 4 million years ago, which is decreasing continuously to the present day.

Keywords Dronning maud · East antarctica Ice sheet (EAIS) · Cosmogenic radionuclides · Last glacial maximum (LGM) · Meltwater runoff

W. Ahmad Baba · J. Kumar Pattanaik (✉)
Department of Geology, Central University of Punjab, Punjab 151001, India

P. Kumar
AMS Division & Geochronology Group, Inter-University Accelerator Centre, New Delhi 110067, India

N. Khare
Ministry of Earth Sciences, Lodhi Road, Prithvi Bhawan, New Delhi 110 003, India

N. Khare (ed.), *Assessing the Antarctic Environment from a Climate Change Perspective*, Earth and Environmental Sciences Library,
https://doi.org/10.1007/978-3-030-87078-2_5

1 Introduction

The Continental ice of Antarctica is separated by the Transantarctic Mountains and created two unequal ice sheets. The West Antarctica Ice Sheet is much smaller than the East Antarctica Ice Sheet (EAIS). The EAIS covering a vast tract of a continental area is an enormous ice mass on the earth's surface (Stonehouse 2002). The EAIS is comprised of several domes (e.g. Dome Fuji, Dome Argus, Dome Circe), reaching > 4.8 km of thickness near Dome Circe and estimated total grounded ice volume is 21.76 $\times 10^6$ km^3 (Lythe and Vaughan 2001; Fretwell et al. 2013; Mackintosh et al. 2014). The EAIS is divided into different parts (e.g., Dronning Maud Land (DML), Enderby Land, Mac. Robertson Land, Wilkes Land, George V Land) based on the continental plateau and regional slope, where mountain chains obstruct large tract of the ice sheet. The EAIS is considered stable than the West Antarctica Ice Sheet and Greenland Ice Sheet; however, recent studies differ (Pingree et al. 2011; Mackintosh et al. 2014). The volume of EAIS is comparable to ~ 53 m of mean seal level (Lythe and Vaughan 2001; Fretwell et al. 2013; Mackintosh et al. 2014); therefore, a minor change in the volume will have a more significant impact on the global sea level. Many unanswered questions about the processes and timescale of the formation and existence of ice sheets in Antarctica. The Continental ice sheet plays a vital role in controlling the earth's climate. Climate modelling suggests that the concentration of CO_2 in the atmosphere is the foremost process for stabilising Antarctica's ice sheet (DeConto and Pollard 2003; Huber et al. 2004; Pollard and DeConto 2009). However, fewer attempts have been made to understand the response of post industrialisation rapid increase of atmospheric CO_2 on ice sheets. Reconstruction of the last 50 years showed significant warming over West Antarctica (0.1 °C per 10 years) and East Antarctica parts (Steig et al. 2009). Paleoglaciation studies on million years' timescale suggest a decrease in the EAIS thickness (Fogwill et al. 2004; Fink et al. 2006; Huang et al. 2008; Strasky et al. 2009; Kong et al. 2010; Di Nicola et al. 2009, 2012; Altmaier et al. 2010; Liu et al. 2010; Lilly et al. 2010). The extent of this decrease and its impact on the global climate are ambiguous. Also, the nature of glacio-eustatic rise, for example, a rapid rise in sea level due to meltwater pulse during the last glacial maximum (LGM), is poorly understood (Clark et al. 2002; Peltier, 2005; Mackintosh et al. 2014). Proxy records from ice cores provide precise and direct methods to analyse Antarctic climate change (Legrand and Mayewski 1997; EPICA Community Members 2006; Mayewski et al. 2009). A continuous record of paleo-temperature and atmospheric compositions is established based on stable isotope study on ice core samples. The most extended history is established up to 800,000 years from Dome Circe (Parrenin et al. 2007). Looking at the vastness of the EAIS and diverse surface and subsurface features, it is difficult to generalise the change observed at one place to the entire ice sheet as the ice sheet's response to the climate change varies with regions. Therefore, each region's glacial history needs to be evaluated using multiple proxies and synthesised for EAIS to have a comprehensive picture at a continental scale. Several studies have been carried out to understand the glacial history based on the available landforms; sediment archives from the lake, coastal and offshore area; ice core data; terrestrial cosmogenic radionuclide (TCN) studies on 'oasis' (ice-free region), nunatak, mountains and glacial debris. In this chapter, the emphasis is given to the Dronning Maud Land region's glacial history based on the study conducted using cosmogenic radionuclides as a proxy.

Cosmogenic radionuclides (CRN) dating techniques have brought a revolution in studying the geomorphic and landscape evolution and the rate at which these processes act on the earth's surface. When the secondary cosmic ray interacts with the rock surface, radionuclides are formed in situ due to spallation reaction. These in situ produced CRNs are used for surface exposure dating. Glacial chronology from thousands to million years is established based on CRN surface exposure ages of glacial landforms, boulders and moraines (Nishiizumi 1993). In a similar timescale, the burial age of sediments or till depositions using CRN provides a chronology for glacial advancement or retreat. Like other methods, this technique has some limitations; however, these limitations can be quickly hindered with detailed field observations, proper sampling strategy and multiple nuclide selections. This age helps to develop the glacial models for ice sheet and valley glaciers. CRN surface exposure dating is only helpful in the ice-free area, mountains, and nunataks present within the ice sheet. In the EAIS, only 1–2% of the site is ice-free and generally found in the coastal zones called 'Oasis' or within Mountain chains. Ages obtained from CRN like ^{14}C from sediment archive also help understand the paleoclimate and glacial history. Several studies were carried out in Dronning Maud Land to understand the glacial history based on CRNs. The literature was reviewed to reconstruct a glacial chronology for the entire region and address a few unanswered questions for future research scope.

1.1 History of Antarctica Glaciation

The ice sheet in Antarctica prevailed since the middle of Tertiary about 35 million years ago, and it is generally agreed that it reached east Antarctica by the Eocene and Oligocene (Barrett et al. 1991, Hambrey et al. 1989; Birkenmayer 1987, 1991; Denton et al. 1991; Prentice and Mathews 1988; Barrera and Huber 1993). However, the commencement and the timing of glaciation required further evaluation. The reconstruction of ice-sheet extent and volume is based on the ocean drilling programmes (ODP), where clay minerals, stable oxygen isotopic concentrations and sediment analysis were carried out on samples collected from the offshore core. Antarctic glaciation's commencement in the middle of Tertiary was possible with the Gondwana breakup, drifting of Antarctica towards poles and formation of ocean gateways or opening of "Darke Passage" (Kennett 1977). Isolation of Antarctica and the development of circumpolar current subsequently led to the cooling and glaciation. Another model suggests that the Antarctica glaciation was initiated due to lower CO_2 concentration in the atmosphere followed by a permanent ice cap due to further lowering CO_2 to a threshold value (DeConto and Pollard 2003; Altmaier et al. 2010). The results from ODP show subtropical to temperate climates on Dronning Maud

Land during Late Cretaceous (Kennett and Barker 1990). Data from the Weddell Sea suggested that Palaeocene's the warmest period (Kennett and Stott 1990; Robert and Kennett 1994). There are no records of ice sheet existence in the Late Cretaceous or Early Tertiary; however, fluctuations of ice sheets in east Antarctica have been reported (Anderson 1999). There was an increase in the ^{18}O concentrations in the deep-sea records during the Eocene period, indicating the growth of ice sheets in Antarctica (Prentice and Mathews 1988, Denton et al. 1991; Abreu and Anderson 1998). Evidence supports ice sheets in east Antarctica during the Oligocene and the spreading of ice in the Ross Sea during Late Oligocene (Denton et al. 1991; Hambrey et al. 1991). However, ice sheet occurrences in west Antarctica are unknown (Birkenmajer 1998; Anderson 1999). Based on the fossil record, earlier studies proposed that temporary large-scale retreat of EAIS during Pliocene (Webb and Harwood 1987); however, the recent studies based on field evidence and numeric modelling do not support the retreat and suggest a stable EAIS during Pliocene (Denton et al. 1984; Sugden et al. 1995; Pollard and DeConto 2009; Altmaier et al. 2010).

1.2 Present-Day Scenario of Antarctica Ice Sheet

The grounding line is an essential indicator of ice sheets' instability, as their changes depict the flow of ice and imbalances with the surrounding ocean. Ocean driven forces have melted various Antarctic glaciers, which have retreated the grounding line rapidly. However, there are limited records to measure imbalance. Between 2010 to 2016, retreat in grounding lines in east Antarctica (3%), Antarctic Peninsula (10%) and West Antarctica (22%) were recorded (Konrad et al. 2018). It has been shown that the retreat has been very swift (25 m yr^{-1}). The loss of grounded ice area has been around 1463 $\pm$ 791 km^2 (Konrad et al. 2018). Satellite altimeter to measure the ice elevation and geometry of the ice were combined with tracking the grounding line movement. The fastest rates have been seen in the Amundsen Sea, while in Pine Island, the grounding line has stabilised possibly due to reduced ocean forcing. According to the ice geometry and satellite measurements, the retreat of grounding lines in west Antarctica, East Antarctica and Antarctica peninsula has been faster after the post-glacial event.

Variations in grounded ice sheets appear due to differences in meltwater runoff, discharge of ice in the ocean and snow accumulation at the surface (Rignot et al. 2011). There has been a reduction in ice thickness in recent times, which has disturbed ice's inland flow. Various satellite techniques complemented with the field measurements and mass balance model have been developed to estimate ice sheet masses' variations (Zwally et al. 2012). It has shown that 2720 $\pm$ 1390 billion tonnes of ice have been lost from Antarctica during from 1992–2017, increasing the sea level by 7.6 $\pm$ 3.9 mm. By this period in west Antarctica, melting has increased from 53 $\pm$ 29 to 159 $\pm$ 26 Billion tonnes per year. However, there are uncertainties in the models showing again in surface mass balance with an average being 5 $\pm$ 46 billion tonnes per year (Shepherd et al. 2018).

1.3 Glacial History: Evidence from Ice Cores

Antarctica's Ice cores indicate changes in the ice volume from the past 4 million years (Petit et al. 1997). Records from the Vostok show a well-built correlation with global ice records. This shows a link between the ice sheets of the northern and southern hemispheres (Petit et al. 1997). However, there are variations in climate and glacial history of Late Quaternary obtained from ice core, terrestrial, offshore records (Jouzel et al. 1987; Petit et al. 1997; Ingólfsson 1998; Anderson 1999; Ingólfsson and Hjort 1999). During the last glacial maxima (LGM), the east Antarctica domes were thinner than the present because the accumulation rates were lower (Jouzel et al. 1989; Siddall et al. 2012). These observations are based on the ice sheet models and the ice core data. However, these changes in ice thickness are poorly known. Ice cores data used to reconstruct elevation using gas content of the bubbles trapped within ice and ice flow models to constraint the accumulation rates. Both the methods have uncertainties in their results; therefore, they should be used carefully for reconstructing glacial event. However, the obtained records of the past ice thickness are consistent with these methods.

2 Dronning Maud Land (DML)

Dronning Maud land is a region in East Antarctica covering an area of 2.7×10^6 km^2 (Fig. 1). In this region, different countries have established permanent research stations operational year-round or sessional to study geology, geodetic, glaciology, geophysics and atmospheric phenomena etc. Some of the essential stations are Maitri (India), Aboa (Finland); Weasands (Sweden); Troll and Tor

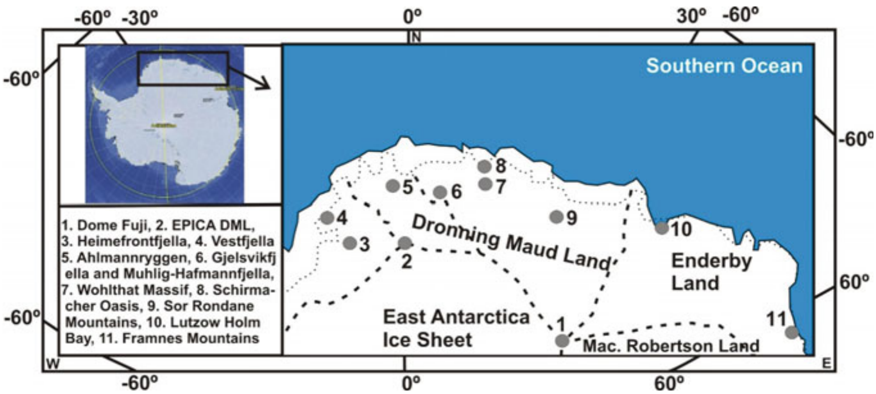

Fig. 1 Location of Dronning Maud Land, East Antarctica and name of the mountain ranges and ice-free regions are given in the diagram (Modified after Mackintosh et al. 2014). Dotted lines indicate the movement of ice mass and slope reduce toward the coastal region

(Norway), Princess Elisabeth Base (Belgium), Neumayer-Station III and Kohnen (Germany), Novolazarevskaya Station (Russia), SANAE IV (South Africa), Asuka, Showa and Dome Fuji Station (Japan).

The Dronning Maud land is dominated by Precambrian gneiss formed between 1 to 1.2 Ga. The mountains in the area are characterised by granitic and crystalline rocks that probably formed 500 to 600 Ma ago during the assemblage of Gondwana land. Younger sedimentary and volcanic rocks are found in the western parts of the region. Borg Massif guards the ice sheet over DML in the west and Yamato Mountain in the east (Pattyn et al. 2010; Mackintosh et al. 2014). The region has thick ice sheets that show downslope towards the coastal part from the continental plateau. Various researchers studied several mountain ranges, nunatak and oasis (ice-free area) located within the DML ice sheet to reconstruct the glacial history of EAIS. The important mountain ranges from west to east are Vestfjella, Heimefrontfjella, Ahlmannryggen, Gjelsvikfjella, Wohlthat Massif (includes Peterman Range, Insel Range, Gruber Mountains and Humboldt Mountains), DallmannBergeandPetermannKetten mountains (south of Wohlthat Massif), and SørRondane Mountains (Fig. 1). Among ice-free areas, Schirmacher oasis, Untersee oasis and coastal oasis in the Lützow-Holm Bay (towards eastern margin of DML ice sheet) were extensively studied for geomorphology, paleoclimate and glacial history. These ice-free regions are home to numerous lakes, Roche Moutonnée, a fossil glacier track filled with boulders, till and moraine deposits.

Striated surfaces and bedrock from nunatak and Roche Moutonnée, erratic's and boulders from fossil glaciers track provide ample opportunities to use cosmogenic radionuclides to measure the surface exposure age, and it can be used for understanding the variation of ice thickness and glacial history. During glacier retreat or thinning and shrinking of the ice sheet, bedrock or boulders are exposed to the cosmic ray, and in situ, cosmogenic radionuclides are produced. Although target nuclides are present in all the rock-forming minerals, quartz is used to measure radionuclides' concentration. The production and decay rate of cosmogenic radionuclides is well established; hence, it calculates bedrock's surface exposure age or boulder. Similarly, sediment archives from the lake deposits and offshore region are used to know the time of deposition using cosmogenic radionuclides, indicating paleoclimate, transport mechanism and paleoenvironmental setting.

2.1 Applications of Cosmogenic Radionuclides (CRN)

Earth and its atmosphere continuously receive solar and galactic cosmic rays. These primary cosmic rays are mainly high-energy (0.01-10^2 GeV) protons and alpha particles. Upon entering into the earth's atmosphere, direct cosmic rays interact with the nuclei of atmospheric elements and produce a cascade of lower energy secondary cosmic rays (mainly neutrons). These secondary cosmic rays further interact with the elements present in the atmosphere and on the earth surface, and in spallation reaction, radioactive isotopes (also called radionuclides) are produced. Radionuclides produced on the earth surface and top layers are called in-situ had CRN (such as ^{10}Be, ^{26}Al, ^{21}Ne etc.) and those made in the atmosphere are called *garden variety* CRN.

Solar cosmic rays are of lower energies and get easily deflected by the geomagnetic field. The atmosphere further causes attenuation. Even at high latitudes, where the geomagnetic deflection is less, solar cosmic rays can penetrate only the topmost layers of the atmosphere and hardly reach the earth's surface their low energy.

Galactic cosmic rays (originating outside the solar system from supernova explosions) are of higher energies and significantly contribute to the in-situ production of ^{10}Be and ^{26}Al. Due to higher energies, GCRs are only partially shielded by the geomagnetic field and reaches earth surfaces after penetrating the whole atmosphere. Major in-situ production channels of ^{10}Be and ^{26}Al on the earth surface are by spallation of neutrons with oxygen (Fig. 2) and silicon, respectively, [$^{16}O\ (n, 4p3n)^{10}Be$, $^{28}Si\ (n, p\ 2n)\ ^{26}Al$ present in quartz mineral].

In-situ ^{10}Be production rate at sea level and latitude $\geq$60°, in the rocks having exposure ages ranging from 11 ka to 4 Ma is estimated between 5.8 to 6.4 atoms per year per gm of quartz (Kubik et al 1998). While, the production rate of ^{26}Al in SiO_2 in terrestrial rocks at sea level and latitude > 60° is about 37 atoms per year per gm of quartz (Kubik et al. 1998), and increases rapidly with altitude to 374 atoms per year per gm of quartz at 3.34 km altitude at 44° N (Nishiizumi et al. 1989).

In areas where the inherited and independent ages coexist, magnitude, rate, and spatial patterns can be revealed from single cosmogenic nuclides. However, by applying two radionuclides (^{10}Be and ^{26}Al) with different half-lives on the same samples, uplift rates can be determined with greater accuracy and confidence (Tuniz 2001). These provide a model that links the erosion and ice dynamics processes. The error ranges lie in $\pm$ 5 – 10% for the surface exposure dating, including systematic and analytical error. CRNs like ^{10}Be, ^{26}Al and ^{14}C are used suitably for the burial age of the sediments/pebble/cobbles depending upon the landforms, local setting and type of sediments.

.

2.2 *Measurement of CRNs*

Cosmogenic ^{10}Be ($T_{1/2}$ = 1.38 Ma) and ^{26}Al ($T_{1/2}$ = 0.72 Ma) in the geological samples are found at a deficient level, and their isotopic ratios (^{10}Be/^{9}Be and ^{26}Al/^{27}Al) ranges between 10^{-11} to 10^{-15}. The measurement of such trace CRNs is challenging and beyond the measurement capabilities of conventional mass spectrometric methods insensitivities and isobaric interferences. Accelerator Mass Spectrometry, in which an individual atom of CRN is counted after removing isobaric and isotopic interferences, is the technique, which can perform such ultrasensitive measurements with very high precision (Kumar et al. 2011, 2014, 2015). The sample processing and AMS measurement methods are described in various references (Kumar et al. 2011, 2014, 2015).

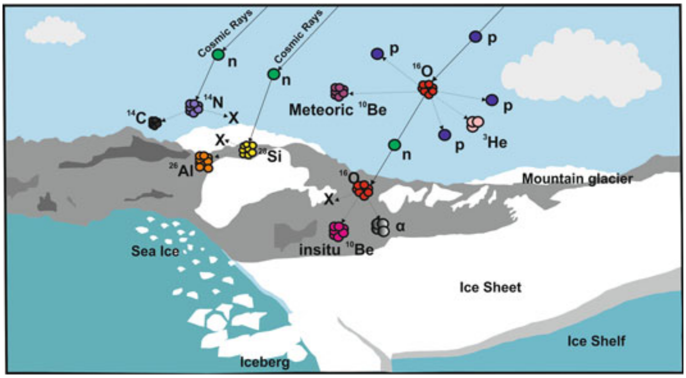

Fig. 2 Showing the in-situ production of Beryllium-10 and Aluminium-26 and production of carbon-14 in the atmosphere (Tuniz 2001; Willenbring and von Blanckenburg 2010)

3 Glacial History of Dronning Maud Land (DML)

Various studies like field observations, ice thickness measurement based on echo sounder, GPR, gravimeter; proxy-based analysis, ice core data, modelling and simulations were used to understand the glacial history of the Droning Maud Land. Most of the field-based studies and data collections were conducted in the continental and ice-free regions as oasis located in the low-lying coastal areas and marginal mountainous areas (Pattyn et al. 1992). The region's present glacial geomorphology is developed due to polycyclic glaciation and deglaciation phases, where deglaciation occurred frequently and for longer durations (Pattyn et al. 1992). Base on-field evidence around the Sor Rondane Mountain region and flow line model, Pattyn et al. (1992) reported that ice thickness was increased by 300–400 m during the last glacial maximum. The previous study based on the ice age model using glaciological and geomorphological evidence also suggests a similar increase in ice thickness of 400 m (Hirakawa and Moriwaki 1990). Based on the ice age simulation, it has been reported that the Grounding line of the Antarctica ice sheet was advanced by 20 km and 100 m thickening of polar ice plateau during that period (Pattyn et al. 1992). The ice cover of DML and EAIS responded slowly to climate change, as reported by Pollard and Deconto (2009) and Huybrechts (1993). In the longer time scale, the recent study using surface exposure dating of nunatak (south-east of Wohlthat Massif) suggest that between 0.75 to 3.57 Ma, the ice surface lowered at a rate less than 1 mm/year (Strub et al. 2015). The authors also did not rule out the possibility of exhumation as it can bring the nunatak above the ice surface. Previous surface exposure study from the same region suggests that Wohlthat Massif was exposed between 1 to 4 Ma ago (Altmaier et al. 2010). However, Strub et al. (2015) argued that this could be due to the thickness of the ice sheet as it was thicker (200–400 m) than today until ~ 0.5 Ma ago or due to the upliftment of that region. Many instance results from recent studies on other parts of the EAIS and for a different period do not converge. Therefore, the glacial history of EAIS is debatable. The effort was made to reconstruct the deglaciation history of Antarctica ice sheet since the Last Glacial Maximum based on the available data from different part of Antarctica by 'The RAISED Consortium' et al. (2014), where a change of the ice thickness and the grounding line position for the different period were discussed. Whereas Mackintosh et al. 2014, described the glacial history for a different location and summarised the changes of EAIS since the Last Glacial Maximum. Previous studies based on the surface exposure ages and burial age of sediments using cosmogenic radionuclides like ^{14}C, ^{10}Be and ^{26}Al were compiled (Table 1), and a sequence of glacial events was established.

3.1 Holocene Period

From the DML region, sparse records from a few oases and nunataks projecting from the ice sheet provides limited information about glacial fluctuation during the Holocene period. Like most Antarctica parts, the grounding line of ice sheets in the DML region was either on the inner shelf or close to the present-day position by 5 ka (The RAISED Consortium et al. 2014). However, in the west part of DML, the grounding line was seaward at the Weddell Sea compared to the present-day position. In the Heimefrontfjella region snow, petrel nests position is lying between 30 and 230 m above the present-day surface, and ^{14}C date of mumiyo sample from basal layer indicate that the since 8700 ± 40 yr B.P. (Lintinen and Nenonen 1997), top of the ice sheet was ~ 30 m above the present surface (Mackintosh et al. 2014). Similarly, mumiyo samples from Ahlmannryggen and Gjelsvikfjella ice-covered ridges in the western part of DML show ^{14}C dates of Holocene age with oldest dates recorded 8330 ± 70 yr B.P. and 3730 ± 80 yr B.P., respectively (Steele and Hiller 1997). These dates considered to be the minimum age of deglaciation of that region. However, other ^{14}C dates from Muhlig-Hafmannfjella, a nearby region, provides older dates and suggesting the thickness of EAIS is close to the present position before LGM (Steele and Hiller 1997; Mackintosh et al. 2014). In the Lützow-Holm Bay region (eastern part of DML), marine fossil samples from raised beach provided two clusters of ^{14}C age, where a sample from Ongul island situated towards north shows ~33–50 ka age, and sample from Skarvsnes and Skallen peninsula towards south shows <7 ka age (Miura et al. 1998; Takada et al. 2003; Mackintosh et al. 2014).

Similarly, samples from other islands in the south show Holocene ages. It was inferred that during the late Pleistocene, EAIS was retreated from the northern part and did not advance during LGM. However, the ice sheet has withdrawn from the southern part after the LGM and region were ice-free during the Holocene. The difference in surface weathering in this area's northern and southern region supports the relative variation in the glaciation history. Another cosmogenic radionuclide dating confirms that the Skarvsnes peninsula had ~ 360 m ice sheet, and it has retreated between 10 and 6 ka ago (Yamane et al. 2011; Mackintosh et al. 2014). Erratic boulders from east Antarctica show that ice sheets reached the present configuration by

Table 1 Cosmogenic radionuclide dating from Dronning Maud Land used for the chronological constraint of glacial history

S.N	Location	Latitude	Longitude	Method	Age (ka)	Reference
1	Dronning Maud Land	69°54.10'S	11°29.61'E	^{14}C	1.55 ± 0.07	Gingele et al. (1997)
2	Gjelsvikfjella	72°09′ S	2° 36′ E	^{14}C	3.73 ± 0.08	Steele and Hiller (1997)
3	Ahlmannryggen	71°50′ S	2° 25′ W	^{14}C	8.33 ± 0.07	
4	Heimefrontjella	74°35'S	11° 0'W	^{14}C	8.7 ± 0.04	Lintinen and Nenonen (1997)
5	Lazarv Sea	70°0.78'S	11°45.30'E	^{14}C	11.14 ± 0.12	Gingele et al. (1997)
6	Schirmacher Oasis	70°45.87' S	11°51.40' E	^{10}Be, ^{26}Al	21 ± 3	Altmaier et al. (2010)
7		70°45.73' S	11°50.79' E	^{10}Be,	22 ± 3	
8	Sør Rondane Mountains	72.2° S	27.8° E	^{10}Be	30 ± 2	Yamane et al. (2015)
9	Gjelsvikfjella	72°9′ S	2°36′ E	^{14}C	31.962 ± 1.7	Steele and Hiller (1997)
10	Lake Unterse (Wohlthat Massif)	71°20′ S	13°27′ E	^{14}C	33.9 ± 3.02	Hiller et al (1988)
11	Schirmacher Oasis	70°45.78' S	11°50.90' E	^{10}Be, ^{26}Al	35 ± 4	Altmaier et al. (2010)
12	Sør Rondane Mountains	72.2° S	27.8° E	^{10}Be, ^{26}Al	35 ± 3	Yamane et al. (2015)
13	Heimefrontjella	74°34′36"S	11°13′24"W	^{14}C	37.4 ± 1.5	Thor and Low (2011)
14	Vestfjella			^{14}C	38.7 ± 1.5	
15	Dallmann Berge	71°45.37'S	10°11.07'W	^{10}Be, ^{26}Al	70 ± 8	Altmaier et al. (2010)
16	Sør Rondane Mountains	72° S	24.9° W	^{10}Be	73 ± 5	Yamane et al. (2015)
17	Dallmann Berge	71°44.4' S	10°9.20' E	^{10}Be, ^{26}Al	81 ± 5	Altmaier et al. (2010)
18	Wohlthat Massif	70°0.78'S	11°45.30'E	TCN	100	

(continued)

Table 1 (continued)

S.N	Location	Latitude	Longitude	Method	Age (ka)	Reference
19	Dallmann Berge	71°45.55’ S	10°11.08’ E	^{10}Be, ^{26}Al	112 ± 7	
20		71°45.3’ S	10°8.6’ E	^{10}Be, ^{26}Al	135 ± 8	
21		71°45.3’ S	10°9.10’ E	^{10}Be, ^{26}Al	166 ± 17	
22		71°45.47’ S	10°11.07’ E	^{10}Be, ^{26}Al	192 ± 11	
23	Schussel/Eckhorner	71° 31.8’ S	11°24.55’ E	^{10}Be, ^{26}Al	196 ± 9	
24	Dallmann Berge	71°45.3’ S	10°10.9’ E	^{26}Al	202 ± 22	
25	Schussel/Seitental	71°36.95’ S	11°28.8’ E	^{10}Be, ^{26}Al	227 ± 11	
26	Untersee Westgrat	71°20’ S	13°24.6’ E	^{10}Be, ^{26}Al	235 ± 11	
27	Dallmann Berge	71°45.86’ S	10°09.78’ E	^{10}Be, ^{26}Al	239 ± 13	
28		71°45.36’ S	10°10.9’ E	^{10}Be	283 ± 15	
29	Untersee Ostgrat	71°21’ S	13°31’ E	^{10}Be, ^{26}Al	339 ± 11	
30		71° 21’ S	13°31’ E	^{10}Be, ^{26}Al	388 ± 14	
31	Sør Rondane Mountains	71.6° S	25.4° E	^{10}Be, ^{26}Al	428 ± 30	Yamane et al. (2015)
32	Dallmann Berge	71°45.42’ S	10°10.9’ E	^{10}Be, ^{26}Al	462 ± 18	Altmaier et al. (2010)
33	Sør Rondane Mountains	72° S	26° E	^{10}Be, ^{26}Al	476 ± 34	Yamane et al. (2015)
34		72° S	24.9° E	^{10}Be	594 ± 43	
35	Untersee Ostgrat	71° 21’ S	13°31’ E	^{10}Be, ^{26}Al	631 ± 19	Altmaier et al. (2010)
36		71° 20’ S	13°24.7’ E	^{10}Be, ^{26}Al	725 ± 35	
37	Sør Rondane Mountains	72° S	26.4° E	^{10}Be	745 ± 57	Yamane et al. (2015)
38	Schussel/Seitental	71°36.95’ S	11°28.8’ E	^{10}Be, ^{26}Al	912 ± 37	Altmaier et al. (2010)

(continued)

Table 1 (continued)

S.N	Location	Latitude	Longitude	Method	Age (ka)	Reference
39	PetermannKetten	71°52.782'S	11°57.364'E	^{10}Be, ^{26}Al	1050 ± 30	
40		71°30.765'S	12°34.481'E	^{10}Be	1150 ± 40	
41		71°53.741'S	11°57.661'E	^{10}Be, ^{26}Al	1180 ± 30	
42		71°24.67' S	12°48.193'E	^{10}Be, ^{26}Al	1530 ± 40	
43	Schussel / Eckhorner	71°31.75' S	11°25.25' E	^{10}Be, ^{26}Al	1760 ± 40	
44		71°31.75' S	11°25.25' E	^{10}Be, ^{26}Al	1760 ± 40	
45	Sør Rondane Mountains	72° S	24.3° E	^{10}Be	1851 ± 116	Yamane et al. (2015)
46	Petermann Ketten	71°53.3' S	11°57.5' E	^{10}Be, ^{26}Al	1920 ± 40	Altmaier et al. (2010)
47	Sør Rondane Mountains	72° S	24.3° E	^{10}Be, ^{26}Al	2980 ± 180	Yamane et al. (2015)
48	Petermann Ketten	71°25.934'S	12°43.88' E	^{10}Be	3000 ± 60	Altmaier et al. (2010)
49		71°50.149'S	12°17.734' E	^{10}Be, ^{26}Al	3770 ± 70	
50	Sør Rondane Mountains	72° S	25° E	TCN	4000	Moriwaki et al. (1991)
51	Petermann Ketten	72°8.362' S	11°30.961' E	^{10}Be	4110 ± 150	Altmaier et al. (2010)

this time. There was considerable thinning of ice sheets between 10 and 5 ka. The Lazarev Sea of east Antarctica has unearthed the processes that controlled the sedimentation over the past 10,000 yr during deglaciation. Lazarev Sea has distinct facies which reveal the environment of deposition with glaciomarine processes. These depositional sequences preserve the retreat of the ice history in this part of the continent. The minimum age of retreat of glaciers obtained from ^{14}C dating is 1550 ± 70 yr B.P. (Gingele et al. 1997).

The dates were obtained from carbonate particles terrestrial areas were exposed by 5 ka. Some areas also indicate fluctuations during Holocene (Gingele et al. 1997). The Nivl Ice Shelf of the Lazarev Sea is situated north of Schirmacher Oasis (Fig. 1), central DML. Laminated sediments from the Nivl Ice Shelf, dated to be 11,140 ± 120 ^{14}C yr B.P. (Gingele et al. 1997) and suggesting deglaciation of continental shelf during early Holocene. Subsequently, proglacial lakes were formed in the Schirmacher oasis (Mackintosh et al. 2014). This ice retreat was continued, and further, Schirmacher Oasis was becoming ice-free, and the proglacial lake became landlocked lakes around 3 ka (Schwab 1998; Phartiyal et al. 2011). However, another study based on surface exposure dating using cosmogenic radionuclide dating and lake sediment dating suggest that Schirmacher oasis was ice-free before LGM (Altmaier et al. 2010).

The substantial recession of ice sheets in east Antarctica arose around 13 cal yrs B.P., and the retreat was swift in Holocene. In West Antarctica, the retreat began at 10 ka. The ice sheets retreated significantly in the eastern and western Antarctica peninsula by the 15 and 10 ka and reached the present state during the Holocene middle. While on the east side, it would have gone by 10 ka (Ingólfsson et al. 2004).

3.2 LGM and Post LGM

The time duration of LGM (Last Glacial Maximum) varies from place to place, and the global chronostratigraphy refers to the time of the event from c. 26.5 to 19 ka B.P. (Clark et al. 2009). The literature term LLGM (Local Last Glacial Maximum) is being used for a specific location (Clark et al. 2009) to explain the last glacial maxima that differ widely. However, global LGM is considered roughly around 20 ka. To avoid such ambiguity, 'The RAISED Consortium et al. (2014) explain Antarctica's glacial history in the different time slices such as 20 ka, 15 ka, 10 ka and 5 ka. Available data shows Antarctica Ice sheet was not at its maximum extent during LGM (Anderson et al. 2002) and shows local variations. The DML region of EAIS shows the variation in glacial history during the LGM period. The glacial-geological data and ice sheet model contradict EAIS elevation changes around the Weddell Sea region during LGM. This region's overall glacial history is diverse compared to other DML sites (Hillenbrand et al. 2012). As per the Weddell Sea marine sediment record, the grounding line's extent is nearly 100 km seaward during 21 ka than the present (Elverhøi 1981; Mackintosh et al. 2014). Several glacio-geomorphological studies were conducted in the Vestfjella, and Heimefrontfjella mountain ranges and some of the result on the past ice thickness and its timing are contradicting (Jonsson 1988; Lintinen 1996; Lintinen and Nenonen 1997; Hattestrand and Johansen 2005). As no chronological constraints are available from the region, based on the field observation like the position of striations and till depositions in the Vestfjella region, the thickness of the ice sheet during LGM was estimated to be 700 m thicker than the present (Hattestrand and Johansen 2005; Mackintosh et al. 2014). However, these results are not supported by the ^{14}C dating of mumyio sample from this region and indicate that since 38,700 ± 1500 yr B.P., the region was ice-free (Thor and Low 2011). Based on the glacio-geomorphological evidence and surface weathering analysis in the Heimefrontfjella area, it has been contended that 100–200 m thicker ice sheet was present during LGM than today. The sediment core samples collected from few lakes situated on the Schirmacher Oasis shows that the region was covered with an ice sheet during LGM (Schwab 1998; Phartiyal et al. 2011); however, it is contradicted by other results. Based on the surface exposure dating using cosmogenic radionuclides in the SorRondane Mountain, it is inferred that the region had ~ 100 m thicker ice sheet during LGM than present-day. Studies on the nunataks from DML shows significantly less or no ice sheet thickening. Additionally, evidence from the ice-core and the ice-sheet model offers a thickness of the ice sheet was 100 m lower than the present during LGM (The RAISED Consortium et al. 2014) in the interior part of the ice sheet.

3.3 Pre LGM

Surface exposure dating using cosmogenic radionuclide from the Wohlthat Massif suggested that the thickness of EAIS has not changed significantly since 100 ka (Altmaier et al. 2010). Similarly, studies indicate that Sor-Rondane Mountain was ice-free since 4 Ma, and however, nunataks from the peripheral parts of this mountain range have become ice-free since 200 ka. Five phases of this region's deglaciation were established based on the surface weathering, where the last stage was dated using cosmogenic radionuclide to be 25 ka (Moriwaki et al. 1991; Nishiizumi et al. 1991; Moriwaki 1992; Ishizuka et al. 1993). There are no advances seen in Schirmacher and Untersee; however, dating and grain size distribution from Lazarev suggests that it may have advanced between 82 ka B.P. (Gingele et al. 1997). Ice sheets in Queen Maud Land were not stable and linked to the ice sheet's interior. There is evidence of changes in the central Antarctic ice sheet during this time scale. The maximum advancement in ice has been sampled from the high altitude Petermann Ketten Mountains. Areas like Untersee, Schussel, on the other hand, suggest that ice sheets were 400 m higher before 0.5 million years. From the data, the impression we get is the steady thinning of the ice sheets; this may be related to the global cooling, which began at the end of the Pliocene. This cooling would have lowered the precipitation rates and, subsequently, Antarctica's ice thickness (Raymo 1992). Other workers Welten et al. 2008 and Höfle 1989, have also supported this.

The evidence from east Antarctica indicates no advance in the ice thickening during the LGM, as is evident from the Sorrondane and Wohlthat Massif. There was a decrease in ice elevation in these areas, as supported by the ice core records. The ice coverage in the last 8 million years is exposed at the high altitude Petermann Ketten Mountains. On the other hand, the ice sheet in Wohlthat Massif had been 200–400 m higher, as shown by the exposure ages of Schussel, Dallmann Berge and Untersee samples. The Eckhorner indicates ice coverage did not exceed 300 m. In general, there is a decrease in ice thickness and exposure of rocks that were buried in ice. This is interpreted as a result of global cooling, which ended in the Pliocene (Raymo 1992). The retreat in the present ice level culminated approximately 0.1 Ma ago. During LGM, the ice level increase was enough to cover the Schirmacher Oasis, as evident from Dallmannberge. A higher concentration of cosmogenic nuclides represents lower rates of erosion from the Peterman Ketten Mountains. These low erosion rates are found in hyper-arid and cold climates. The dates obtained from this area were the first attempt.

4 Melt Water Pulse (MWP)

Several meltwater pulses (MWP) were recorded since the LGM period. There was about an 18 m increase in sea level due to MWP1a during 14.7 to 13.3 ka (Deschamps et al. 2012). The pattern in sea level rise indicates a considerable contribution from the Southern hemisphere. However, the recent data from ice sheet models and ice core records show that only 10 m of ice was locked equally to the eustatic level during LGM (Golledge et al. 2012; Whitehouse et al. 2012; Mackintosh et al. 2011). Mackintosh et al. 2011 suggest that the volume of EAIS increased by 1 m, excluding the embayments of Weddell and Ross seas which is equal to the eustatic level of LGM. This indicates a total 10% contribution from Antarctic ice sheets as shown by the ice sheet models (Golledge et al. 2012; Mackintosh et al. 2011; Whitehouse et al. 2012; Pollard and DeConto 2009). It is not straight forward to understand the contribution of EAIS to the MWP1a, as the volume of ice is small and deglaciation was slow and late. There is evidence of a small donation to MWP1a from Amery and Lambert (Verleyen et al. 2005). There is no clear evidence on how significantly EAIS contributed to MWP1a due to the lack of data or insufficient data constraining or modelling techniques, which needs to be assessed.

5 Marine Isotope Records

Marine isotope records are essential for understanding the Quaternary climate globally (Lisiecki and Raymo 2005; Golledge et al. 2012). Although isotopic records are also affected by the deep-water temperatures (Shackleton 1967), these records are used as a proxy since 1960 to decipher global ice volume. The LGM in Antarctica is not well established; however, it is assumed that it may have occurred during the marine isotope stage 2 (MIS-2). In east Antarctica, maximum extension occurred by 17 ka and 10.7 ka B.P. at Prydz and Mac's coasts. Robertson Land. In the Antarctic Peninsula, the LGM occurred after 30 ka B.P. (Sugden and Clapperton 1980). Recent studies suggest that the Wisconsin ice sheet would have formed by 20 to18 ka (Bentley and Anderson 1998), indicate ice sheets were higher before 35 ka.

In the same way, ice sheets in the Weddell Sea were higher before 26 ka. However, Hjort et al. (2003) indicate the maximum extension in ice occurred before MIS-3 in the western part of the Weddell Sea. Late Quaternary ice distribution suggests Antarctic sea ice in winter advanced towards the present polar zone by MIS-2. During MIS-3, there were several climatic warmings known as Dansgaar and Oeschgerevents (D.O.), between 60 and 27 ka. D.O. events are a period of transition from cold to mild conditions followed by the return of stadial conditions (Dansgaard et al. 1993).

In MIS-3, D.O. events were regular is unclear why they were so frequent. These events were absent during the LGM. Ice cores from Greenland show the rise of 8–16 °C followed by a cooling period before the temperatures returned to stadial values. These transitions have also been indicted by the North Atlantic Ocean (Huber et al. 2006; North GRIP-Members 2004). Marine records suggest that interstadials had higher sea temperature and ocean deep ventilation than stadia. There is a scarcity of information on the east Antarctic ice sheet during MIS-3. Ice models suggest that EAIS expanded during MIS-3 in comparison to the Holocene. However, the field evidence contradicts the modelling evidence and indicates that ice sheets did not advance than the present. Cosmogenic results show that there were areas, which were ice-free for most of the marine isotope stage-3. The last glacial cold cycle has the most prolonged period at around 118 ka. Interglacial period MIS 5-e is at 115 ka (Shackleton et al. 2002 and 2003). The cold cycle of the last glacial had two various complex stages during MIS 4 and 2. Temperature and dust records of Antarctica also indicate this. The average temperature in Antarctica reached −10.2 °C and −10.6 °C for marine isotope stage 4 and 2. These two are divided by the warm interglacial of MIS-3. The millennial-scale variability indicated by Antarctic and Greenland ice core records (Blunier et al. 1998; Markle et al. 2017). Hughes et al. 2013 reported the asynchronies in the glacial cycles, mainly in Asia, where they advanced during the yearly glaciation cycle (Astakhov 2018; Larsen et al. 2006; Svendsen et al. 2004; Vorren et al. 2011). There is evidence of thicker ice sheets in Antarctica before LGM, while at the centre of east Antarctica, there was no thicker ice at LGM than at present (Lilly et al. 2010). Some marine oxygen records indicate the global volume of ice was higher in marine isotope stage 6 than MIS-2 (Roucoux et al. 2011; Shackleton 1987). This is supported by Shakun et al. (2015) for global sea level. However, data obtained by Lisiecki and Raymo (2005) show that MIS-2 has higher ^{18}O records than MIS-6. However, temperature effects may hide the ice volume because, during MIS-6, sea surface temperatures were warmer than MIS-5d-2. This has allowed the supply of moisture to drive the extent of ice masses more in other glacial periods. The distribution of ice before LGM was different from LGM. Eurasia had more ice masses before LGM. Similarly, North America had smaller ice masses before LGM compared to the LGM (Rohling et al. 2017). The pre-glacial maximum peak occurred around 140 ka (Colleoni et al. 2016; Stirling et al. 1998; Raisbeck et al. 2014).

6 Summary

Grounding line in most Antarctica parts was near the present shelf before 20 ka except in the Ross and the Weddell Sea. Besides, the extent of ice reached before 20 ka in some places while recession had started at this time (Hillenbrand et al. 2014). The geological and marine data shows considerable ice by 20 ka in the Weddell Sea's continental shelf. From the east and west Antarctica, the data is limited. Half of the ice that has been grounded in the Ross Sea comes from east Antarctica (Anderson et al. 2014). Radiocarbon dates show that the recession of ice sheets started before the LGM. Some parts of East Antarctica reached the present shelf margin by this time (Mackintosh et al. 2014). The sediments of the MIS-3 suggest that several areas were ice-free at this time. Likewise, in Dronning Maud land, there are sparse or no evidence of ice thickening during LGM. Ice sheet and ice core models show the ice domes were possibly 100 m lower than at present. Striated bedrock, till, and organic deposits like mumiyo provide evidence for changes in the past and the dynamics of EAIS. Various workers' analysis was combined, which showed that a 600 m high ice sheet existed 4 million years ago, decreasing continuously to the present day. The question is how much mean sea level is expected to rise under different climatic scenario's (Bindoff et al. 2007). By reconstructing the glacial history of EAIS could help address these questions and understand the more direct dates required from this region. Surface exposure dating using cosmogenic radionuclide proved to be a potential technique to date the deglaciation phase. From Dronning Maud Land, more dates need to be generated to establish a detailed glacial chronology. The work is in progress to establish chronology in DML with the sample collected during 36th Indian Scientific Expedition to Antarctica by one of the authors.

Acknowledgements JKP is thankful to the present and former Vice-chancellor, Central University of Punjab, Bathinda and the Director, NCPOR, Goa, Ministry of Earth Sciences, for support and help during the 36th Indian Scientific expedition to Antarctica. JKP also thankful to Ms. Amrutha K. for her help to prepare diagram for this chapter.

References

Abreu VS, Anderson BJ (1998) Glacial eustasy during the Cenozoic: sequence stratigraphic implications. Am Asso Petrol Geol Bull 82(7):1385–1400

Altmaier M, Herpers U, Delisle G, Merchel S, Ott U (2010) Glaciation history of Queen Maud Land (Antarctica) reconstructed from in-situ produced cosmogenic ^{10}Be, ^{26}Al and ^{21}Ne. Polar Sci 4(1):42–61

Anderson JB (1999) Antarctic marine geology. Cambridge University Press, Cambridge

Anderson JB, Shipp SS, Lowe AL, Wellner JS, Mosola AB (2002) The Antarctic Ice Sheet during the Last Glacial Maximum and its subsequent retreat history: a review. Quat Sci Rev 21:49–70

Anderson JB, Conway H, Bart PJ, Witus AE, Greenwood SL, McKay RM, Hall BL, Ackert RP, Licht K, Jakobsson M, Stone JO (2014) Ross Sea paleo ice sheet drainage and deglacial history during and since the LGM. Quat Sci Rev 100:31–54

Astakhov VI (2018) Late Quaternary glaciation of the northern Urals: a review and recent observations. Boreas 47(2):379–389

Barrera E, Huber BT (1993) Eocene to Oligocene oceanography and temperatures in the Antarctic Indian Ocean. In: The Antarctic paleoenvironment: a perspective on global change: American Geophysical Union Antarctic Research Series, vol 60, pp 49–65

Barrett PJ, Hambrey MJ, Robinson PR (1991) Cenozoic glacial and tectonic history from CIROS-1, McMurdo Sound. In: International symposium on antarctic earth sciences, vol 5, pp 651–656

Bentley MJ, Anderson, JB (1998) Glacial and marine geological evidence for the ice sheet configuration in the weddell sea–antarctic peninsula region during the last glacial maximum. Antarct Sci 10(3):309–325

Bindoff NL, Willebrand J, Artale V, Cazenave A, Gregory JM, Gulev S, Shum CK (2007) Observations: oceanic climate change and sea level. ClimateChange 385–432

Birkenmajer K (1991) Tertiary glaciations in the South Shetlands Islands, West Antarctica: evaluation of data. In: International symposium on Antarctic earth sciences, vol 5, pp 629–632

Birkenmajer K (1998) Geology of Volcanic Rocks (? Upper Cretaceous-Lower Tertiary) at Potter Peninsula, King George Island (South Shetland Islands, West Antarctica. Bull Pol Acad Sciences Earth Sci. Earth Sciences 46(2):147–155

Birkenmajer KRZYSZTOF (1987) Oligocene-Miocene glaciomarine sequences of King George Island (South Shetland Islands), Antarctica. PalaeontologiaPolonica 49(1):9-36

Blunier T, Chappellaz J, Schwander J, Dällenbach A, Stauffer B, Stocker TF, Raynaud D, Jouzel J, Clausen HB, Hammer CU, Johnsen S (1998) Asynchrony of antarctic and greenland climate change during the last glacial period. Nature 394(6695):739–743

Clark PU, Mitrovica JX, Milne GA, Tamisiea ME (2002) Sea-level fingerprinting as a direct test for the source of global meltwater pulse I.A. Science 295(5564):2438–2441

Clark PU, Dyke AS, Shakun JD, Carlson AE, Clark J, Wohlfarth B, McCabe AM (2009) The last glacial maximum. Science 325(5941):710-714

Colleoni F, Wekerle C, Näslund JO, Brandefelt J, Masina S (2016) Constraint on the penultimate glacial maximum Northern Hemisphere ice topography (~140 kyrsBP). Quatern Sci Rev 137:97–112

Dansgaard W, Johnsen SJ, Clausen HB, Dahl-Jensen D, Gundestrup NS, Hammer CU, Bond G (1993) Evidence for general instability of past climate from a 250-kyr ice-core record. Nature 364(6434):218-220

DeConto RM, Pollard D (2003) Rapid Cenozoic glaciation of Antarctica induced by declining atmospheric CO_2. Nature 421(6920):245–249

Denton GH, Prentice ML, Kellogg DE, Kellogg TB (1984) Late Tertiary history of the Antarctic ice sheet: evidence from the Dry Valleys. Geology 12(5):263–267

Denton GH, Prentice ML, Burckle LH (1991) Cainozoic history of the Atlantic ice sheet. The geology of Antarctica, pp 365–433

Deschamps P, Durand N, Bard E, Hamelin B, Camoin G, Thomas AL, Yokoyama Y (2012). Ice-sheet collapse and sea-level rise at the Bølling warming14,600years ago. Nature 483(7391):559-564

Di Nicola L, Strasky S, Schlüchter C, Salvatore MC, Akçar N, Kubik PW, Baroni C (2009). Multiple cosmogenic nuclides document complex Pleistocene exposure history of glacial drifts in Terra Nova Bay (northern Victoria Land, Antarctica). *Quaternary Research*, *71*(1), 83-92

Di Nicola L, Baroni C, Strasky S, Salvatore MC, Schlüchter C, Akçar N, Wieler R (2012). Multiple cosmogenic nuclides document the East Antarctic Ice Sheet's stability in northern Victoria Land since the Late Miocene (5–7 Ma). *Quat Sci Revs*, *57*, 85-94

Elverhøi A (1981) Evidence for a late Wisconsin glaciation of the Weddell Sea. Nature 293(5834):641–642

EPICA Community Members (2006) One-to-one coupling of glacial climate variability in Greenland and Antarctica. Nature 444(7116):195

Fink D, McKelvey B, Hambrey MJ, Fabel D, Brown R (2006) Pleistocene deglaciation chronology of the Amery Oasis and Radok Lake, northern Prince Charles Mountains, Antarctica. Earth Planet Sci Lett 243(1-2):229-243

Fogwill CJ, Bentley MJ, Sugden DE, Kerr AR, Kubik PW (2004) Cosmogenic nuclides 10Be and 26Al imply limited Antarctic Ice Sheet thickening and low erosion in the Shackleton Range for> 1. Geology 32(3):265–268

Fretwell P, Pritchard HD, Vaughan DG, Bamber JL, Barrand NE, Bell R, Catania G (2013) Bedmap2: improved ice bed, surface and thickness datasets for Antarctica. The Cryosphere 7(1):375–393

Gingele FX, Kuhn G, Maus B, Melles M, Schöne T (1997) Holocene ice retreat from the Lazarev Sea shelf. East Antarctica. Cont Shelf Res 17(2):137–163

Golledge NR, Fogwill CJ, Mackintosh AN, Buckley KM (2012) Dynamics of the last glacial maximum Antarctic ice-sheet and its response to ocean forcing. Proc Natl Acad Sci 109(40):16052–16056

Hambrey MJ, Larsen B, Ehrmann WU (1989) Forty million years of Antarctic glacial history yielded by Leg 119 of the Ocean Drilling Program. PolarRecord 25(153):99–106
Hambrey MJ, Ehrmann W, Larsen B (1991) Cenozoic glacial record of the Prydz Bay continental shelf, East Antarctica. In: Barron J, Larsen B et al (eds.) Proc. ODP, Sci. Results, College Station, TX. (Ocean Drilling Program), vol 119, pp 77–132; vol 119, pp 77–132
Hättestrand C, Johansen N (2005) Supraglacial moraines in Scharffenbergbotnen, Heimefrontfjella, Dronning Maud Land, Antarctica-significance for reconstructing former blue ice areas. Antarct Sci 17(2):225
Hillenbrand CD, Melles M, Kuhn G, Larter RD (2012) Marine geological constraints for the Antarctic Ice Sheet's grounding-line position on the southern Weddell Sea shelf at the Last Glacial Maximum. Quatern Sci Rev 32:25–47
Hillenbrand CD, Bentley MJ, Stolldorf TD, Hein AS, Kuhn G, Graham AG, Larter RD (2014) Reconstruction of changes in the Weddell Sea sector of the Antarctic Ice Sheet since the Last Glacial Maximum. Quat Sci Revs 100:111-136
Hiller A, Wand U, Kampf H, Stackebrandt W (1988) Occupation of the Antarctic continent by petrels during the past 35000 years - inferences from a ^{14}C study of stomach oil deposits. Polar Biol 9:69–77
Hirakawa K, Moriwaki K (1990) Former ice sheet based on the newly observed glacial landforms and erratics in the central SørRondane Mountains, East Antarctica. Proc NIPR Symp Antarct Geosci 4:41e54
Hjort C, Ingólfsson Ó, Bentley MJ, Björck S (2003) The late pleistocene and holocene glacial and climate history of the antarctic peninsula region as documented by the land and lake sediment records-a review. Antarct Penins Clim Var: Hist Paleoenviron Perspect 79:95–102
Höfle HC (1989) The glacial history of the Outback Nunataks area in western North Victoria Land. Geologisches Jahrbuch. Reihe e, Geophysik 38:335–355
Huang F, Liu X, Kong P, Fink D, Ju Y, Fang A, Na C (2008) Fluctuation history of the interior East Antarctic Ice Sheet since mid-Pliocene. Antarct Sci 20(2):197
Huber C, Leuenberger M, Spahni R, Flückiger J, Schwander J, Stocker TF, Jouzel J (2006) Isotope calibrated Greenland temperature record over Marine Isotope Stage 3 and its relation to CH4. Earth Planet Sci Lett 243(3-4):504-519
Huber M, Brinkhuis H, Stickley CE, Döös K, Sluijs A, Warnaar J, Williams GL (2004) Eocene circulation of the Southern Ocean: was Antarctica kept warm by subtropical waters? Paleoceanography 19(4):1-12
Hughes PD, Gibbard PL, Ehlers J (2013) Timing of glaciation during the last glacial cycle: evaluating the concept of a global 'Last Glacial Maximum (LGM). Earth Sci Rev 125:171–198
Huybrechts P (1993) Formation and disintegration of the AntarcticIce Sheet. Ann Glaciol 20:336–340
Ingólfsson Ó, Hjort C (1999) The Antarctic contribution to Holocene global sea-level rise. Polar Res 18(2):323–330
Ingólfsson Ó (2004) Quaternary glacial and climate history of Antarctica. In: Developments in Quaternary sciences, vol 2, pp 3–43. Elsevier
Ingólfsson Ó, Hjort C, Berkman PA, Björck S, Colhoun E, Goodwin ID, Prentice ML (1998) Antarctic glacial history since the Last Glacial Maximum: an overview of the record on land. Antarct Sci 10:326-344
Ishizuka H, Shiraishi K, Moriwaki K (1993) Geological Map of Bergersenfjella. In: AntarcticGeological Map Series. National Institute for Polar Research, Tokyo
Jonsson S (1988) Observations on the physical geography and glacial history of the Vestfjellanunataks in western Dronning Maud Land. Stockholms Universitet, Naturgeografiska Institutionen, Antarctica
Jouzel J, Lorius C, Petit JR, Genthon C, Barkov NI, Kotlyakov VM, Petrov VM (1987) Vostok ice core: a continuous isotope temperature record over the last climatic cycle (160,000 years). Nature 329(6138):403–408

Jouzel J, Raisbeck G, Benoist JP, Yiou F, Lorius C, Raynaud D, Kotlyakov VM (1989) A comparison of deep Antarctic ice cores and their implications for climate between 65,000 and 15,000 years ago. Quat Res 31(2):135-150

Kennett JP (1977) Cenozoic evolution of Antarctic glaciation, the circum-Antarctic ocean, and their impact on global paleoceanography. J Geophys Res 82(27):3843–3860

Kennett JP, Barker PF (1990) Latest Cretaceous to Cenozoic climate and oceanographic developments in the Weddell Sea, Antarctica: an ocean-drilling perspective. In: Proceedings of the ocean drilling program, scientific results, vol 113, pp 937–960

Kennett JP, Stott LD (1990) Proteus and Proto-Oceanus: ancestral Paleogene oceans as revealed from Antarctic stable isotopic results; ODP Leg 113. In: Proceedings of the ocean drilling program, scientific results, vol 113, pp 865–880). Ocean Drilling Program College Station, TX

Kong P, Huang F, Liu X, Fink D, Ding L, Lai Q (2010) Late Miocene ice sheet elevation in the Grove Mountains, East Antarctica, inferred from cosmogenic ^{21}Ne–^{10}Be–^{26}Al. Global Planet Change 72(1–2):50–54

Kubik PW, Ivy-Ochs S, Masarik J, Frank M, Schlucher C (1998) ^{10}Be and ^{26}Al production rates deduced from an instantaneous event within the dendro-calibration curve, the landslide of Kofels, Otz Valley, Austria. Earth Planet Sci Lett 161(1–4):231–241

Kumar P, Pattanaik J, Ojha S, Gargari S, Joshi R, Roonwal G, Kanjilal D (2011) ^{10}Be measurements at IUAC-AMS facility. J Radioanal Nucl Chem 290(1):179-182

Kumar P, Pattanaik JK, Khare N, Chopra S, Yadav S, Balakrishnan S, Kanjilal D (2014) Study of ^{10}Be in the sediments from the Krossfjorden and Kongsfjorden Fjord System, Svalbard. J Radioanal Nucl Chem 302(2):903–909

Kumar P, Chopra S, Pattanaik JK, Ojha S, Gargari S, Joshi R, Kanjilal D (2015) A new AMS facility at Inter-University Accelerator Centre, New Delhi. Nucl Instrum Methods Phys Res Sect B 361:115–119

Konrad H, Shepherd A, Gilbert L, Hogg AE, McMillan M, Muir A, Slater T (2018) The net retreat of Antarctic glacier grounding lines. Nat Geosci 11(4):258–262

Larsen E, KJaeR KH, Demidov IN, Funder S, Grøsfjeld K, Houmark-Nielsen MICHAEL, Lysa A (2006) Late Pleistocene glacial and lake history of northwestern Russia. Boreas 35(3):394-424

Legrand M, Mayewski P (1997) Glaciochemistry of polar ice cores: a review. Rev Geophys 35(3):219–243

Lilly K, Fink D, Fabel D, Lambeck K (2010) Pleistocene dynamics of the interior East Antarctic ice sheet. Geology 38(8):703–706

Lintinen PETRI (1996) Evidence for the former existence of a thicker ice sheet on the Vestfjella-nunataks in western Dronning Maud Land, Antarctica. Bull-Geol Soc Finl 68:85–98

Lintinen P, Nenonen J (1997) Glacial history of the Vestfjella and Heimefrontfjellanunatak ranges in western Dronning Maud Land, Antarctica. Geological Evolution and Processes. Terra Antarctica Publications, Sienna, The Antarctic Region, pp 845–852

Lisiecki LE, Raymo ME (2005) A Pliocene-Pleistocene stack of globally distributed benthic δ18O records, Paleoceanography, 20, PA1003

Liu X, Huang F, Kong P, Fang A, Li X, Ju Y (2010) History of ice sheet elevation in East Antarctica: Paleoclimatic implications. Earth Planet Sci Lett 290(3–4):281–288

Lythe MB, Vaughan DG (2001) BEDMAP: a new ice thickness and subglacial topographic model of Antarctica. J Geophys Res: Solid Earth 106(B6):11335–11351

Mackintosh A, Golledge N, Domack E, Dunbar R, Leventer A, White D, …& Gore D(2011) The retreat of the East Antarctic ice sheet during the last glacial termination. Nat Geosci 4(3):195–202

Mackintosh AN, Verleyen E, O'Brien PE, White DA, Jones RS, McKay R, Miura H (2014) Retreat history of the East Antarctic Ice Sheet since the last glacial maximum. Quat Sci Revs 100:10-30

Markle BR, Steig EJ, Buizert C, Schoenemann SW, Bitz CM, Fudge TJ, Sowers T (2017) Global atmospheric teleconnections during Dansgaard–Oeschger events. Nat Geosci 10(1):36-40

Mayewski PA, Meredith MP, Summerhayes CP, Turner J, Worby A, Barrett PJ, Bromwich D (2009) State of the Antarctic and Southern Ocean climate system. Rev Geophys 47(1):RG1003

Miura H, Maemoku H, Seto K, Moriwaki K (1998) Late Quaternary East Antarctic melting event in the Soya Coast region based on stratigraphy and oxygen isotopic ratio of fossil molluscs. Polar Geosci 11:260–274

Moriwaki K (1992) Late Cenozoic glacial history in the Sφr-Rondane Mountains, East Antarctica. In: Recent progress in Antarctic earth science, 661–667

Moriwaki K, Hirakawa K, Matsuoka N (1991) Weathering stage of till and glacial history of the central SørRondane Mountains, East Antarctica. Proc NIPR Symp Antarct Geosci 5:99–111

Nishiizumi K, Winterer EL, Kohl CP, Klein J, Middleton R, Lal D, Arnold JR (1989) Cosmic ray production rates of 10Be and 26Al in quartz from glacially polished rocks. J Geophys Res: Solid Earth 94(B12):17907–17915

Nishiizumi K, Kohl CP, Arnold JR, Klein J, Fink D, Middleton R (1991) Cosmic ray produced 10Be and 26Al in Antarctic rocks: exposure and erosion history. Earth Planet Sci Lett 104(2–4):440–454

Nishiizumi K, Kohl CP, Arnold JR, Dorn R, Klein I, Fink D, Lal D (1993) Role of in situ cosmogenic nuclides ^{10}Be and ^{26}Al in the study of diverse geomorphic processes. Earth Surf Process Landfs 18(5):407-425

North Greenland Ice-Core Project (NorthGRIP) Members (2004) High-resolution climate record of the Northern Hemisphere reaching into the last Glacial Interglacial Period. Nature 431:147–151

Parrenin F, Barnola JM, Beer J, Blunier T, Castellano E, Chappellaz J, Kawamura K (2007) The EDC3 chronology for the EPICA Dome C ice core. Clim Past 3(3):485–497

Pattyn F, Decleir H, Huybrechts P (1992) Glaciation of the central part of the SørRondane, Antarctica: glaciological evidence. In: Recent progress in Antarctic earth science. Tokyo: Terra Scientific Publishing Company, pp 669–678

Pattyn F, Matsuoka K, Berte J (2010) Glacio-meteorological conditions in the vicinity of the Belgian Princess Elisabeth Station, Antarctica. Antarct Sci 22(1):79-10

Peltier WR (2005) On the hemispheric origins of meltwater pulse 1a. Quatern Sci Rev 24(14–15):1655–1671

Petit JR, Basile I, Leruyuet A, Raynaud D, Lorius C, Jouzel J, …& Davis M(1997) Four climate cycles in Vostok ice core. Nature 387(6631):359–360

Pingree K, Lurie M, Hughes T (2011) Is the East Antarctic ice sheet stable? Quatern Res 75(3):417–429

Phartiyal B, Sharma A, Bera SK (2011) Glacial lakes and geomorphological evolution of Schirmacher Oasis, East Antarctica, during late quaternary. Quatern Int 235(1–2):128–136

Pollard D, DeConto RM (2009) Modelling West Antarctic ice sheet growth and collapse through the past five million years. Nature 458(7236):329–332

Prentice ML, Matthews RK (1988) Cenozoic ice-volume history: development of a composite oxygen isotope record. Geology 16(11):963–966

Raisbeck LB, Xiao H, Liang F, Akers PD, Brook GA, Dennis WM, Edwards RL (2014) A stalagmite record of abrupt climate change and possible Westerlies-derived atmospheric precipitation during the Penultimate Glacial Maximum in northern China. Palaeogeogr Palaeoclim Palaeoecol 393:30–44

Raymo ME (1992) Global climate change: a three million year perspective. In: Start of a glacial, pp 207–223. Springer, Berlin, Heidelberg

Rignot E, Mouginot J, Scheuchl B (2011) Ice flow of the Antarctic ice sheet. Science 333(6048), 1427–1430

Robert C, Kennett JP (1994) The antarctic subtropical humid episode at the Paleocene-Eocene boundary: clay-mineral evidence. Geology 22(3):211–214

Rohling EJ, Hibbert FD, Williams FH, Grant KM, Marino G, Foster GL, Webster JM (2017) Differences between the last two glacial maxima and implications for ice-sheet, δ^{18}O, and sea-level reconstructions. Quatern Sci Rev 176:1–28

Roucoux KH, Tzedakis PC, Lawson IT, Margari V (2011) Vegetation history of the penultimate glacial period (Marine isotope stage 6) at Ioannina, north-west Greece. J Quat Sci 26(6):616–626

Schwab MJ (1998) Reconstruction of the Late Quaternary climatic and environmental history of the Schirmacher Oasis and the Wohlthat Massif (East Antarctica). BerichtezurPolarforschung 293:128

Shackleton NJ (1987) Oxygen isotopes, ice volume and sea level. Quatern Sci Rev 6(3–4):183–190

Shackleton NJ, Chapman M, Sánchez-Goñi MF, Pailler D, Lancelot Y (2002) The classic marine isotope substage 5e. Quatern Res 58(1):14–16

Shackleton NJ, Sánchez-Goñi MF, Pailler D, Lancelot Y (2003) Marine isotope substage 5e and the Eemian interglacial. Global Planet Change 36(3):151–155

Shackleton N (1967) Oxygen isotope analyses and Pleistocene temperatures re-assessed. Nature 215(5096):15–17

Shakun JD, Lea DW, Lisiecki LE, Raymo ME (2015) An 800-kyr record of global surface ocean δ18O and implications for ice volume-temperature coupling. Earth Planet Sci Lett 426:58–68

Shepherd A, Ivins E, Rignot E, Smith B, Van Den Broeke M, Velicogna I, Nowicki S (2018) Mass balance of the Antarctic Ice Sheet from 1992 to 2017. Nature 558:219-222

Siddall M, Milne GA, Masson-Delmotte V (2012) Uncertainties in elevation changes and their impact on Antarctic temperature records since the last glacial period. Earth Planet Sci Lett 315:12–23

Steig EJ, Schneider DP, Rutherford SD, Mann ME, Comiso JC, Shindell DT (2009) Warming of the Antarctic ice-sheet surface since the 1957 International Geophysical Year. Nature 457(7228):459–462

Steele WK, Hiller A (1997) Radiocarbon dates of snow petrel (Pagodromanivea) nest sites in central Dronning Maud Land, Antarctica. Polar Record 33(184):29-38

Stirling CH, Esat TM, Lambeck K, McCulloch MT (1998) Timing and duration of the Last Interglacial: evidence for a restricted interval of widespread coral reef growth. Earth Planet Sci Lett 160(3–4):745–762

Stonehouse B (2002) Encyclopaedia of Antarctica and the southern oceans. Wiley

Strasky S, di Niocola L, Baroni C, Salvatore MC, Baur H, Kubik PW, Wieler R (2009) Surface exposure ages imply multiple low-amplitude Pleistocene variations in the East Antarctic ice sheet, Ricker Hills, Victoria Land. Antarct Sci 21(1):59-69

Strub E, Wiesel H, Delisle G, Binnie SA, Liermann A, Dunai TJ, Coenen HH (2015) Glaciation history of Queen Maud Land (Antarctica)–New exposure data from nunataks. Nucl Instrum Methods Phys Res Sect B: Beam Interact Mater Ats 361:599-603

Sugden DE, Clapperton CM (1980) West Antarctic ice sheet fluctuations in the Antarctic Peninsula area. Nature 286(5771):378–381

Sugden DE, Denton GH, Marchant DR (1995) Landscape evolution of the Dry Valleys, Transantarctic Mountains: tectonic implications. J Geophys Res: Solid Earth 100(B6):9949–9967

Svendsen JI, Alexanderson H, Astakhov VI, Demidov I, Dowdeswell JA, Funder S, Hubberten HW (2004) Late Quaternary ice sheet history of northern Eurasia. Quatern Sci Rev 23(11–13):1229–1271

Takada M, Tani A, Miura H, Moriwaki K, Nagatomo T (2003) ESR dating of fossil shells in the Lützow-Holm Bay region, East Antarctica. Quatern Sci Rev 22:1323–1328

The RAISED Consortium, Bentley MJ, Cofaigh CO, Anderson JB, Conway H, Davies B, Graham AG, Zwartz (2014). A community-based geological reconstruction of Antarctic Ice Sheet deglaciation since the Last Glacial Maximum. Quat Sci Revs 100:1-9

Thor G, Low M (2011) The snow petrel's persistence (Pagodromanivea) in Dronning Maud Land (Antarctica) for over 37,000 years. Polar Biol 34(4):609–613

Tuniz C (2001) Accelerator mass spectrometry: ultra-sensitive analysis for global science. Radiat Phys Chem 61(3–6):317–322

Verleyen E, Hodgson DA, Milne GA, Sabbe K, Vyverman W (2005) Relative sea-level history from the Lambert Glacier region, East Antarctica, and its relation to deglaciation and Holocene glacier readvance. Quatern Res 63(1):45–52

Vorren TO, Landvik JY, Andreassen K, Laberg JS (2011) Glacial history of the Barents Sea region. In: Developments in quaternary sciences, vol 15, pp 361–372. Elsevier

Webb PN, Harwood DM (1987) Terrestrial flora of the Sirius Formation: its significance for Late Cenozoic glacial history. Antarct J Unit States 22(4):7–11

Welten KC, Folco LUIGI, Nishiizumi K, Caffee MW, Grimberg A, Meier MMM, Kober F (2008) Meteoritic and bedrock constraints on the glacial history of Frontier Mountain in northern Victoria Land, Antarctica. Earth Planet Sci Lett 270(3-4):308-315

Whitehouse PL, Bentley MJ, Le Brocq AM (2012) Antarctica's deglacial model: geological constraints and glaciological modelling as a basis for a new Antarctic glacial isostatic adjustment model. Quatern Sci Rev 32:1–24

Willenbring JK, von Blanckenburg F (2010) Meteoric cosmogenic Beryllium-10 adsorbed to river sediment and soil: Applications for earth-surface dynamics. Earth-Sci Rev 98(1–2):105–122

Yamane M, Yokoyama Y, Miura H, Maemoku H, Iwasaki S, Matsuzaki H (2011) The last deglacial history of Lützow-Holm Bay, East Antarctica. J Quat Sci 26(1):3–6

Yamane M, Yokoyama Y, Abe-Ouchi A, Obrochta S, Saito F, Moriwaki K, Matsuzaki H (2015) Exposure age and ice-sheet model constraints on Pliocene East Antarctic ice sheet dynamics. Nat Commun 6. https://doi.org/10.1038/ncomms8016

Zwally HJ, Giovinetto MB, Beckley MA, Saba JL (2012) Antarctic and Greenland drainage systems. In: GSFC cryospheric sciences laboratory. http://icesat4.gsfc.nasa.gov/cryo_data/ant_grn_drainage_systems.php